



115
838
THS




3 1293 00876 1607

This is to certify that the
thesis entitled
**AN ALTERNATIVE METHOD FOR DETERMINING
THE DAMAGE BOUNDARY CURVE
OF A SHOCK-SENSITIVE PRODUCT**

presented by
GARY ALLEN LIEBERMAN

has been accepted towards fulfillment
of the requirements for
MASTER degree in PACKAGING


Major professor

Date FEBRUARY 5, 1991

LIBRARY
Michigan State
University

PLACE IN RETURN BOX to remove this checkout from your record.
 TO AVOID FINES return on or before date due.

DATE DUE	DATE DUE	DATE DUE
JAN 11 2000 _____	_____	_____
_____	_____	_____
_____	_____	_____
_____	_____	_____
_____	_____	_____
_____	_____	_____
_____	_____	_____

MSU Is An Affirmative Action/Equal Opportunity Institution

c:\cinc\dstdue.pm3-p.1

AN ALTERNATIVE METHOD FOR DETERMINING
THE DAMAGE BOUNDARY CURVE
OF A SHOCK-SENSITIVE PRODUCT

By

Gary Allen Lieberman

A THESIS

Submitted to
Michigan State University
in partial fulfillment of the requirements
for the degree of

MASTER OF SCIENCE

School of Packaging

1991

ABSTRACT

AN ALTERNATIVE METHOD FOR DETERMINING THE DAMAGE BOUNDARY CURVE OF A SHOCK-SENSITIVE PRODUCT

By

Gary Allen Lieberman

Determining the fragility of a shock-sensitive product is the first step towards meeting packaging requirements. The primary goal of fragility testing is to develop the product's Damage Boundary Curve. Problems with the current methodology which uses a vertical shock machine to construct the Damage Boundary Curve are examined. An alternative method is proposed which does not require the use of a shock machine. With the aid of minimal instrumentation and a computer program, the fragility of a shock-sensitive product can be inexpensively determined from simple drop tests.

Copyright by
Gary Allen Lieberman
1991

Dedication

This thesis is dedicated to Shelia, Jeremy, and Tim.

ACKNOWLEDGMENTS

I wish to thank Dr. Gary James Burgess, Professor - School of Packaging, who served as my major professor and was instrumental in the development of this thesis. Without Dr. Burgess's instruction, this thesis would not have been possible.

I also wish to extend my gratitude to my two other committee members: Dr. Susan Elizabeth Selke, Professor - School of Packaging, and Dr. George E. Mase, Professor - Department of Metallurgy, Mechanics, and Materials Science.

TABLE OF CONTENTS

LIST OF TABLES	viii
LIST OF FIGURES	ix
Chapter One: Introduction and Overview of Shock and Fragility	1
I. Impact and Damage	2
A. The Shock Pulse	2
B. Fragility and the Damage Boundary Curve ...	4
II. The Vertical Shock Machine, ASTM D 3332 and the Conventional Method of DBC Construction ...	15
A. The Vertical Shock Machine	15
B. ASTM D 3332 - Mechanical Shock Fragility of Products Using Shock Machines and the Conventional Method of DBC Construction ...	19
III. Limitations of Damage Boundary Theory and Shock Machines	20
A. Damage Boundary Theory	20
B. Limitations of the Shock Machine	20
Chapter Two: An Alternative Method for Determining the DBC of a Shock-Sensitive Product ..	27
I. The Alternate Method	27
Chapter Three: Simulation Test Results, Sensitivity Analysis, Experimental Procedure, and Concluding Comments	36
I. Simulation Test Results	36
II. Sensitivity Analysis	38
III. Experimental Procedure	43

TABLE OF CONTENTS CONTINUED

IV. Concluding Comments	48
List of References	49
Appendix A	50
Appendix B	51
Appendix C	52
Appendix D	53
Appendix E	55
Appendix F	56
Appendix G	57

LIST OF TABLES

Table 1.	Combinations of peak acceleration and duration (Columns 1 and 5) or peak acceleration and velocity change (Columns 5 and 6) for <u>half-sine</u> shocks to the product which just damage the critical element	9
Table 2.	Combinations of peak acceleration and duration (Columns 1 and 5) or peak acceleration and velocity change (Columns 5 and 6) for <u>square-wave</u> shocks to the product which just damage the critical element	12
Table 3.	Shock Machine Calibration Chart for 2 ms Half-Sine Programmers (bare table)	18
Table 4.	Ability of the Program to Predict $f_{ce} = 20$ Hz and $G_{cr} = 100$ G's Using Border-line Damage Half-Sine Shock Pairs from Appendix D	37
Table 5.	Ability of the Program to Predict the Properties of f_{ce} and G_{cr} for Various Critical Elements	38
Table 6.	Effect on f_{ce} and G_{cr} Determinations When V_{prod} and G_{prod} Values of Shock Pairs #12 and #43 from Appendix D Are Perturbed 10%.	42

LIST OF FIGURES

Figure 1.	Three parameters associated with a sinusoidal shock pulse	2
Figure 2.	Rectangular (a) and Trapezoidal (b) shock pulses	3
Figure 3.	Model of product protected by a cushion	5
Figure 4.	DBC for half-sine shocks to a product containing a critical element with $f_{ce} = 20$ Hz and $G_{ce} = 100$ G's	11
Figure 5.	DBC for square-wave shocks to a product containing a critical element with $f_{ce} = 20$ Hz and $G_{ce} = 100$ G's	13
Figure 6.	An example of a vertical shock machine	16
Figure 7.	ASTM D 3332 method of fairing a square-wave shock pulse	21
Figure 8.	ASTM D 3332 method of fairing a half-sine shock pulse	23
Figure 9.	Haversine shock pulse	39

Chapter One: Introduction and Overview of Shock and Fragility

The primary function of packaging is to preserve and protect the product as it is transported through the distribution environment. Specifically, a function of packaging materials is to reduce the intensity of an external shock transmitted from the environment to the product inside the package. Due to the high cost of package cushioning materials, it is important that the fragility of a shock-sensitive product be accurately determined so that packaging costs can be minimized.

The conventional method used to determine the fragility of a shock-sensitive product relies on a vertical shock machine with a programmable impact surface. The purpose of this thesis is to eliminate the need for a shock machine in fragility testing and to promote an alternative method that is much less expensive.

First, the need for fragility testing of shock-sensitive products and the role of shock machines for this purpose are examined. Next, the capabilities of a conventional shock machine are explored. Finally, an alternative method is presented that requires minimal instrumentation to determine the damage boundary curve for a shock-sensitive product.

I. Impact and Damage

A. The Shock Pulse

The potential for damage to a product in an impact is related to certain features of the shock pulse to the product. The shape of the shock pulse in most situations is very nearly sinusoidal as shown in Figure 1. It has become customary to concentrate on the peak acceleration, the pulse duration, and the velocity change. The peak acceleration is usually expressed in "G's"; a reported value of 20 G's for example means that the peak acceleration is 20 times that of normal gravity, $g = 386.4 \text{ in/sec}^2$.

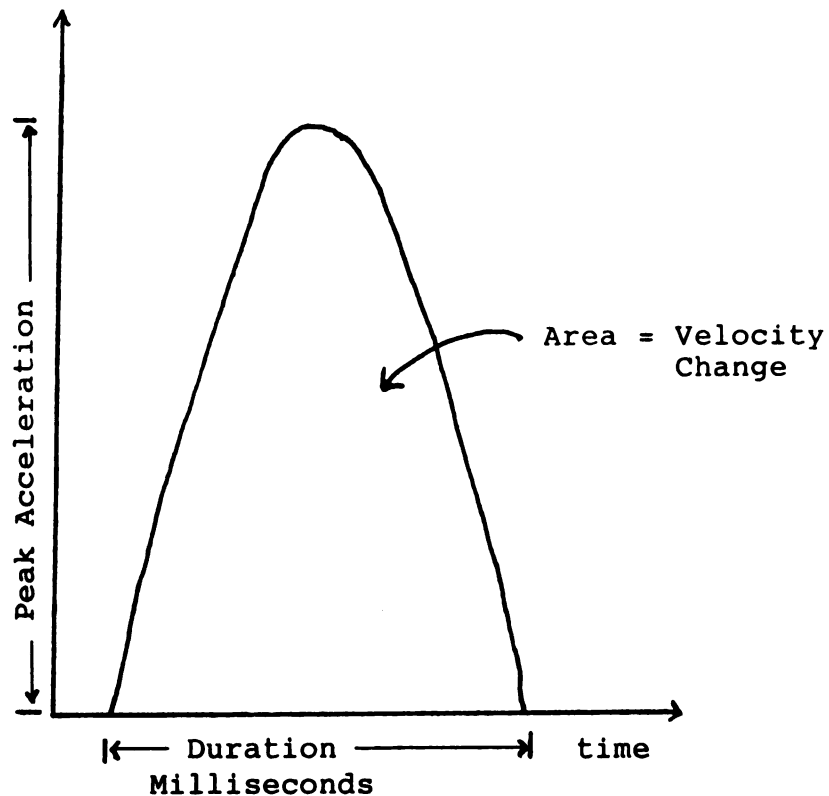


Figure 1. Three parameters associated with a sinusoidal shock pulse.

A less common shock pulse which can be produced by a vertical shock machine is the "trapezoidal-wave" and its relative, the "square-wave", both of which are shown in Figure 2.

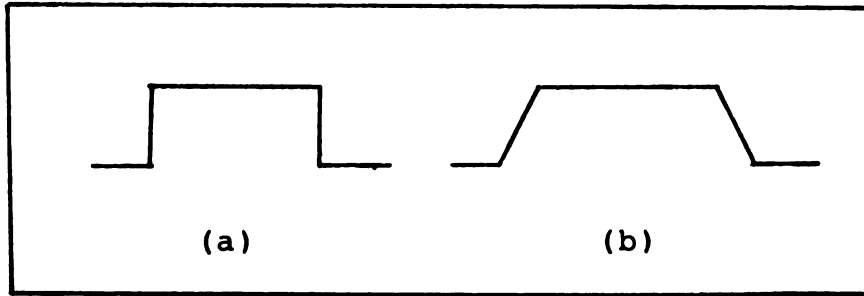


Figure 2. Rectangular (a) and Trapezoidal (b) shock pulses.

All of these pulses are characterized by the same three parameters; peak acceleration, pulse duration, and velocity change. The three can be related to each other using the definition for instantaneous acceleration;

$$\text{acc} = \frac{dv}{dt} \quad (1)$$

where acc is the acceleration, dv is the differential change in velocity, and dt is the differential change in time.

Rearranging and integrating over the duration T of the shock pulse gives

$$\int_0^T dv = \int_0^T \text{acc} * dt \quad (2)$$

The integral on the left in equation(2) is the velocity change Δv and the integral on the right is the area under the acceleration vs time curve. Expressing this area as a shape factor multiplied by the base and height of the waveform gives

$$\Delta v = (\text{shape factor}) * (\text{peak acceleration}) * (\text{duration}) \quad (3)$$

where the shape factor is 1.0 for a square-wave and $2/\pi = 0.636$ for a half-sine wave. The velocity change in equation (3) is the sum of magnitudes of the impact and rebound velocities.

B. Fragility and the Damage Boundary Curve

It is not obvious which features of the shock pulse are associated with damage. Is it peak acceleration, duration, Δv , or a combination of these? Since inertial forces are directly proportional to acceleration, it has become customary to associate the fragility of a product with the maximum acceleration that it can withstand without breaking [Newton, 1976]. Unfortunately, this is too simplistic. The duration of the shock is equally important. Consequently, a complete assessment of the fragility of a product must account for the combinations of peak acceleration, duration, and velocity change which damage a product [Brandenburg and Lee, 1985].

The analysis begins with a model of the product as a rigid mass containing a critical element which is elastically

connected to the product, as indicated in Figure 3 [Newton, 1976]. The product is assumed to fail when the critical element breaks.

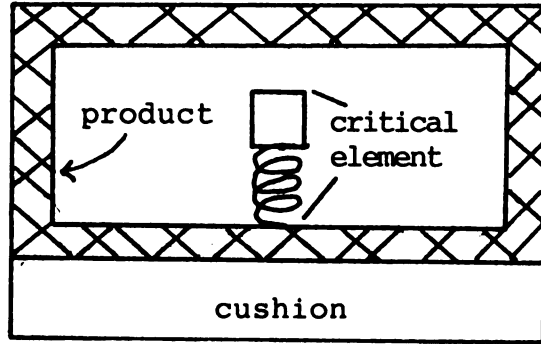


Figure 3. Model of product protected by a cushion.

Four important assumptions are made about the nature of the critical element: (1) it is lightweight compared to the bulk of the product; (2) it acts as an ideal (linear) spring/mass system; (3) it fails when its acceleration exceeds a certain amount regardless of duration; and (4) it is the most fragile component of the product.

The shock that is transmitted to the critical element in an impact is not the same as the shock to the product. Depending on the duration of the shock,

$$G_{ce} = A_m * G_{prod} \quad (4)$$

where G_{ce} is the shock transmitted to the critical element,

A_m is an amplification factor, and G_{prod} is the shock to the product. A_m is a function of the ratio of the natural frequency of the critical element f_{ce} to the natural frequency of the critical element f_{ce} to the natural frequency of the product on its cushion f_{prod} . The value of A_m also depends on the shape of the shock pulse to the product.

For half-sine shock pulses, A_m is determined by [Brandenburg and Lee, 1985]:

$$A_m = \frac{2*(f_{ce}/f_{\text{prod}})*\cos(\pi*f_{ce}/2*f_{\text{prod}})}{1 - (f_{ce}/f_{\text{prod}})^2} \quad (5)$$

when $f_{ce}/f_{\text{prod}} \leq 1.0$;

$$A_m = f_{ce}/f_{\text{prod}} * \sin\left[\frac{\pi*N*2}{f_{ce}/f_{\text{prod}} + 1}\right] \quad (6)$$

when $f_{ce}/f_{\text{prod}} > 1.0$

where N is the integer between 1.0 and $(1 + f_{ce}/f_{\text{prod}})/2$ which maximizes A_m

A table of A_m versus frequency ratio for half-sine shocks is shown in Appendix A.

For square-wave shock pulses, A_m is determined by [Brandenburg and Lee, 1985]:

$$A_m = 2*\sin\left[\frac{f_{ce}*\pi}{2*f_{\text{prod}}}\right] \quad (7)$$

when $f_{ce}/f_{\text{prod}} \leq 1.0$;

$$A_m = 2.0 \text{ when } f_{ce}/f_{\text{prod}} > 1.0 \quad (8)$$

A table of A_m versus frequency ratio for square-wave shocks is shown in Appendix B.

To illustrate the use of equation (4) in determining the complete fragility picture, consider a hypothetical product containing a critical element which has a natural frequency of 20 Hz and a fragility of 100 G's (see Figure 3). The product itself could be a television set and the critical element a transistor or integrated circuit mounted on a circuit board inside the TV.

In the following simulation, the product will be "subjected" to a series of cushioned drops which produce half-sine shock pulses with different durations. The combinations of peak G and duration which cause the critical element to fail will be tabulated. For each shock, it is necessary that the natural frequency of the product on its cushion be known in order that the correct amplification factor be selected to obtain the acceleration of the critical element. As the duration of each shock varies, the natural frequency of the product on its cushion does also. Since the duration of the shock is one half of the natural period of vibration [Brandenburg and Lee, 1985], the natural frequency (cycles per second) is

$$f_{\text{prod}} = 1/(2 \cdot \text{duration}) \quad (9)$$

In Table 1, the duration of the shock is arbitrarily chosen and the corresponding shock and velocity change to the product which just damage the critical element are calculated. Column 1 contains the shock duration chosen and Column 2 shows the natural frequency of the product on its cushion for the given duration obtained from equation(9). Column 3 lists the ratio of f_{ce}/f_{prod} . Since the natural frequency of the critical element is known to be 20 Hz, this ratio is always equal to $20/f_{prod}$. Column 4 contains the amplification factor for this frequency ratio using either equations(5) and (6) or the table in Appendix A. Column 5 shows the required shock to the product using equation(4). Since the critical element is known to break at 100 G's (commonly depicted as $G_{cr} = 100$ G's where G_{cr} refers to the critical acceleration of the critical element), G_{prod} is always equal to $100/A_m$. Finally, the last column shows the corresponding velocity change in accordance with equation(3),

$$\Delta v = \text{shape factor} \times \text{acc} \times \text{duration} \quad (3)$$

$$\Delta v = 0.636 * (\text{Column 5} * 386.4) * (\text{Column 1} / 1000)$$

Table 1. Combinations of peak acceleration and duration (Columns 1 and 5) or peak acceleration and velocity change (Columns 5 and 6) for half-sine shocks to the product which just damage the critical element.

(1) duration (ms)	(2) f_{prod} (Hz)	(3) $f_{\text{ce}}/f_{\text{prod}}$	(4) A_m	(5) G_{prod}	(6) ΔV (in/sec)
100.0	5.00	4.00	1.268	78.9	1941.0
50.0	10.00	2.00	1.732	57.7	710.0
40.5	12.35	1.62	1.769	56.5	563.0
25.0	20.00	1.00	1.571	63.7	391.0
20.0	25.00	0.80	1.373	72.8	358.0
15.0	33.33	0.60	1.102	90.7	335.0
10.0	50.00	0.40	0.771	129.7	319.0
5.0	100.00	0.20	0.396	252.5	311.0
2.5	200.00	0.10	0.200	500.0	307.5

These results merit some discussion. It is interesting to note that despite the fact that the critical element's fragility is 100 G's, the smallest shock to the product that is needed to damage the critical element is only 56.5 G's because the largest A_m possible is 1.769. Also, as $f_{\text{ce}}/f_{\text{prod}}$ becomes small, the value of A_m approaches $2*f_{\text{ce}}/f_{\text{prod}}$. This result follows directly either from taking the limit of equation(5) for small frequency ratios or by inspection from the table in Appendix A. This leads to the result that G_{prod} becomes inversely proportional to the duration; from equations (4) and (9),

$$G_{\text{prod}} = \frac{G_{\text{ce}}}{A_m} = \frac{G_{\text{ce}}}{2*f_{\text{ce}}} = \frac{G_{\text{ce}}*f_{\text{prod}}}{2*f_{\text{ce}}} = \frac{G_{\text{ce}}*1.0}{2*f_{\text{ce}}*2*d} = \frac{G_{\text{ce}}}{4*f_{\text{ce}}*d} \quad (10)$$

where d represents the shock duration.

This also leads to the result that the velocity change approaches a critical lower limit; from equations (3) and (10),

$$\Delta v_{cr} = \frac{2 \cdot (G_{prod}) \cdot (duration)}{\uparrow \uparrow} = \frac{1}{2 \cdot \uparrow \uparrow} * \frac{G_{cr} * 386.4}{f_{ce}} \quad (11)$$

This limiting value of velocity change is referred to as "the critical velocity change", Δv_{cr} . The significance of Δv_{cr} is that if the actual velocity change in a drop is less than this value, the critical element will not break regardless of the shock to the product. The reason for this is that the duration of the shock is so short that the critical element cannot fully respond to the shock.

The results in Table 1 are shown graphically in Figure 4. The locus of points on G_{prod} vs Δv_{prod} axes representing combinations of shock and velocity change to the product which just damage the critical element is known as the Damage Boundary Curve (DBC). The smallest product velocity change required to damage the critical element is the critical velocity change Δv_{cr} and the smallest shock to the product required to damage the critical element is the critical acceleration G_{cr} . Note that the DBC in Figure 4 is for half-sine shocks to the product (Figure 1).

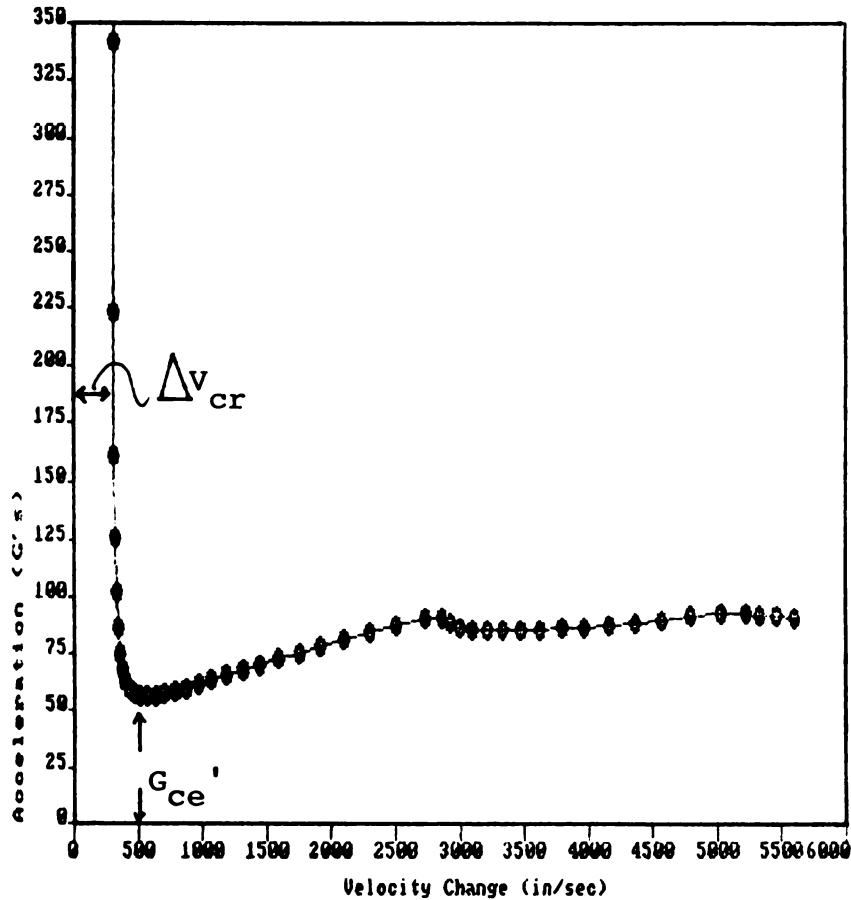


Figure 4. DBC for half-sine shocks to a product containing a critical element with $f_{ce} = 20$ Hz and $G_{cr} = 100$ G's.

The most important conclusion to be drawn from this example is that a knowledge of the fragility G_{cr} and natural frequency f_{ce} of the critical element completely determine the DBC. This was expected since it is the critical element which is assumed to break. The two most notable features of the DBC, Δv_{cr} and G_{cr}' , for half-sine shocks to the product are from equation(11) and the table in Appendix A,

$$\Delta v_{cr} = 61.5 * G_{cr} / f_{ce} \quad (11)$$

$$G_{ce}' = G_{cr}/1.769 \quad (12)$$

Again, information about the critical element determines both these quantities. For this particular product, $\Delta v_{cr} = 307.5$ in/sec and $G_{ce}' = 56.5$ G's.

For shocks to the product which are not half-sine, the shape of the DBC is different. The procedure for tabulating the information is the same as for Table 1 except that a different A_m is used in Column 4 and a different shape factor in Column 6. For example, for square-wave shocks as in Figure 2a, the results in Columns 5 and 6 in Table 1 would change as a result of using A_m from either equations(7) and (8) or from the table in Appendix B and a shape factor of 1.0 in Column 6. The results are shown in Table 2 and Figure 5.

Table 2. Combinations of peak acceleration and duration (Columns 1 and 5) or peak acceleration and velocity change (Columns 5 and 6) for square-wave shocks to the product which just damage the critical element.

(1) duration (ms)	(2) f_{prod} (Hz)	(3) f_{ce}/f_{prod}	(4) A_m	(5) G_{prod}	(6) Δv (in/sec)
100.0	5.00	4.00	2.000	50.00	1932.00
50.0	10.00	2.00	2.000	50.00	966.00
40.5	12.35	1.62	2.000	50.00	782.46
25.0	20.00	1.00	2.000	50.00	483.00
20.0	25.00	0.80	1.902	52.58	406.31
15.0	33.33	0.60	1.619	61.77	358.00
10.0	50.00	0.40	1.176	85.03	328.57
5.0	100.00	0.20	0.618	161.80	312.75
2.5	200.00	0.10	0.313	319.62	307.50

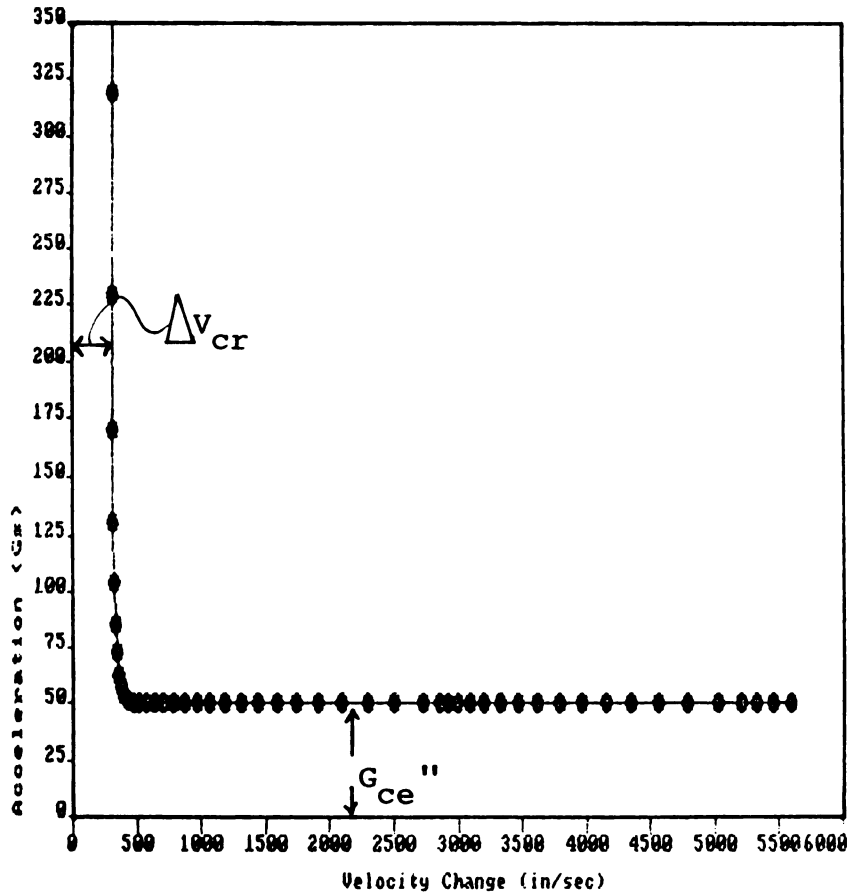


Figure 5. DBC for square-wave shocks to a product containing a critical element with $f_{ce} = 20$ Hz and $G_{cr} = 100$ G's.

Again, note that a knowledge of the properties of the critical element (G_{cr} and f_{ce}) completely determines the shape of the DBC for a specified shape of the shock pulse to the product. For a square-wave shock, the shape of the DBC is much simpler, a rectangle with a rounded corner. The critical velocity change and critical acceleration are obtained as follows: for extremely short duration shocks, f_{prod} is large and f_{ce} is small. From equation(7), A_m approaches a value of $A_m = \pi(f_{ce}/f_{prod})$ so that G_{prod} approaches a value of $G_{prod} =$

$(G_{cr} * f_{prod}) / (\gamma * f_{ce})$. The velocity change then approaches a limiting value of

$$\Delta v_{cr} = 61.5 * G_{cr} / f_{ce} \quad (13)$$

which is exactly the same as for half-sine shocks (equation (11)). Since the largest A_m is 2.00, the critical acceleration for a square-wave shock to the product is

$$G_{ce}'' = G_{cr} / 2 \quad (14)$$

The DBC for square-wave shocks in Figure 5 is by far the more commonly used description of fragility since square-wave shocks to the product are considered to be the most severe [Newton, 1976] even though they rarely occur in practice.

The problem with the approach used to generate either DBC is that it requires a knowledge of the properties of the critical element. If the product were a light bulb and critical element the filament inside, it would be difficult to obtain information about G_{cr} and f_{ce} . This is usually true of all products which have the model in Figure 3. Information pertaining to the critical element is nonexistent. What is needed therefore is a procedure which eliminates the need to know anything about the critical element and provides for the construction of the DBC directly. For square-wave shocks, this is all made possible by the fact that the shape of the DBC is basically rectangular. The entire curve is therefore determined by only two numbers, Δv_{cr} and $G_{cr} / 2$. These two

values may be obtained by subjecting the product to drop tests on a shock machine which can produce both long and short duration square-wave shocks as outlined below. In fact, for short duration shocks, it is not necessary that the shape be a square-wave since the critical velocity change is the same for both square and half-sine shocks (see equations(11) and (13)). The procedure for performing this type of fragility test is summed up in a standard method which will be covered next.

II. The Vertical Shock Machine, ASTM D 3332 and the Conventional Method of DBC Construction

A. The Vertical Shock Machine

The conventional method, ASTM D 3332: Mechanical-Shock Fragility of Products Using Shock Machines, that is used to determine a product's DBC utilizes a vertical shock machine, an example of which is illustrated in Figure 6. The purpose of the shock machine is to control the nature and intensity of the shock by adjusting the hardness of the impact surface (which controls the shock duration) and by varying the table drop height (which controls the velocity change). Dual hydraulic hoists lift the table up the guide columns. When the table is lifted to the desired drop-height, drop controls release pneumatic brakes that hold the table and it falls (under the force of gravity minus friction effects due to the guide posts) onto the programmers. After each drop, the pneumatic brakes stops the table after it rebounds off the programmer surface to prevent multiple impacts.

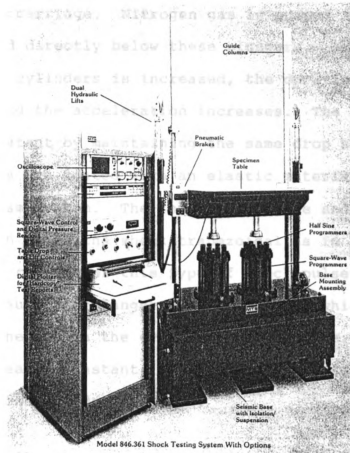


Figure 6. An example of a vertical shock machine.

When a half-sine shock pulse is desired, the table is programmed to fall onto 'half-sine programmers' that are made of a special epoxy resin. As the table drop height increases, both the acceleration and velocity change increase while the duration of the shock pulse is kept very nearly constant at about 0.002 seconds.

When a square-wave shock pulse is desired, the table is programmed to fall onto the 'gas programmers'. As indicated in Figure 6, the table has two piston-type plungers attached

to its undercarriage. Nitrogen gas is pumped into two cylinders located directly below these plungers. As the gas pressure in the cylinders is increased, the duration of the shock decreases and the acceleration increases. The velocity change is held constant by maintaining the same drop height.

The plungers are coated with an elastic material which act as a spring/mass system. The shock pulse rise and fall is nearly linear which makes the shock trapezoidal as in Figure 2b.

The plateau region for this type of shock pulse is intended to be flat because the plunger travel is small which changes the volume of the gas in the cylinders very little. Since the gas volume is nearly constant, so is the gas pressure which leads to nearly constant deceleration.

An oscilloscope may be used to record the shock pulse delivered to the product using an accelerometer attached to the shock machine table. A waveform analyzer may be used to determine the peak acceleration, duration, and velocity change. A hard copy of the signal can be obtained by simply tracing the signal with tracing paper, photographing the signal, or by means of a digital plotter.

Not shown in Figure 6 are electronic filters whose function is to condition the resulting complex signal so that the shock wave can be conveniently displayed. The shock pulse that results whenever the table drops onto the programmers is complex because of "ringing effects" superimposed onto the shock pulse by the table, hydraulic lift cables, and guide

column vibrations. The filtered signal is a very smooth curve.

Finally, the shock machine is attached to a seismic base whose purpose is to absorb the shock and isolate it from the shock machine area.

Shock machines may be supplied with calibration tables from the manufacturer. A calibration table would be required if a shock machine were purchased without an oscilloscope or waveform analyzer. An example of a calibration table is shown in Table 3.

Table 3. Shock Machine Calibration Chart for 2 ms Half-Sine Programmers (bare table)

Drop Height (inches)	Δv (in/sec)	G's
2	55	160
5	91	305
10	128	455
14	153	560
17	169	620

The information presented in Table 3 is only a portion of the entire calibration chart. A calibration chart also exists for the gas programmer as well.

The shock machine is used to determine the DBC of a product in conjunction with ASTM D 3332. The application of this standard in determining a product's DBC is the subject of the next section.

B. ASTM D 3332 - Mechanical Shock Fragility of Products Using Shock Machines and the Conventional Method of DBC Construction

A widely used standard which delineates the procedure for fragility testing using a shock machine is ASTM D 3332.

A summary of the procedure follows.

The test begins with determining the critical velocity change needed to damage the product. Since Δv_{cr} is associated with short duration shocks, the product is mounted onto the shock machine table and the table is programmed to fall onto the plastic programmers. Beginning with a low drop (typically 2"), the table is dropped and the product is inspected for damage. If there is none, the height of each subsequent drop is increased until the product is damaged. The velocity change which just causes damage to the product is defined to be the critical velocity change for the product.

In the second part of the test, a new product is mounted onto the table of the shock machine and the table is raised to a height that will produce a velocity change which will exceed the critical velocity change by at least 57%. The gas pressure is gradually increased for subsequent drops until the product is damaged. When the product becomes damaged, the acceleration that just causes damage is defined to be the critical acceleration of the product, and is loosely referred to as its fragility.

As indicated in Figure 5, the critical velocity change and critical acceleration completely determine the DBC since the entire DBC can be effectively described by the intersection of two lines, the locations of which are determined by the critical velocity change and critical acceleration. In the next section, limitations of damage boundary theory and shock machines will be examined.

III. Limitations of Damage Boundary Theory and Shock Machines

A. Damage Boundary Theory

The damage boundary curve has been constructed under the assumption that a product contains a fragile critical element(s) that behaves as an ideal spring/mass system(s). However, many types of products do not have critical elements. An example is an apple. Furthermore, even if a product has a critical element, it may not behave as an ideal linear spring/mass system. Therefore, the DBC for the product may not have the shape shown in Figure 5. As a consequence, cushioning which is selected based on product fragility shown in the curve may lead to unexplained product failure. This may be attributed to the inability of the model to account for fatigue failure as a result of repeated shocks. Even if the product can be adequately modeled as a rigid mass containing an ideal critical element, there are still practical problems associated with using the shock machine to deduce the DBC.

B. Limitations of the Shock Machine

When a shock machine is used to produce a square-wave, it is assumed that the gas programmer generates the shock pulse shown in Figure 2a. Upon closer examination, however, the shock wave that is produced by the gas programmer is clearly not square in shape but appears as shown in Figure 7. The complex shape complicates the velocity change and peak acceleration determinations.

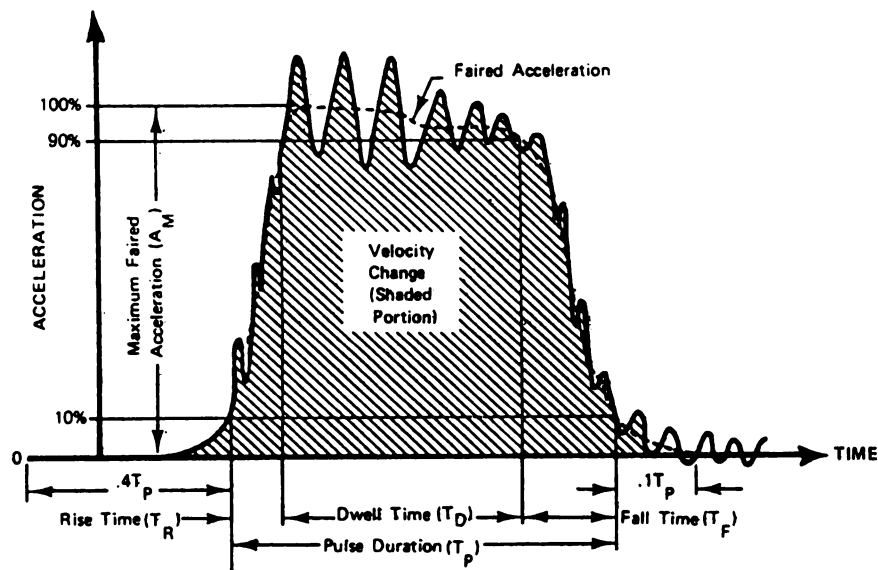


Figure 7. ASTM D 3332 method of fairing a square-wave shock pulse.

If a waveform analyzer is not used during the test, then determining the peak acceleration and velocity change may be difficult due to the presence of ringing effects discussed earlier. According to ASTM D 3332, either signal conditioning (electronic filtration) or "fairing the pulse" can be used to smooth out the shock pulse so that the values of velocity

change and peak acceleration can be conveniently determined. ASTM's method for fairing the pulse however is very confusing. It begins by stating that two horizontal lines be drawn through the shock pulse at levels that purportedly represent 90% and 10% of the maximum faired acceleration. But how can a technician get 90% and 10% of something that they do not know yet (the maximum faired acceleration is what they are looking for!)? Nonwithstanding, ASTM D 3332 goes on to state that two perpendicular lines are then drawn from the intersection of these two lines and the shock pulse curve at the bottom of the shock pulse. As indicated by Figure 7, these two sets of vertical lines define the dwell time T_D and Pulse Duration T_P . T_P and T_D are used to construct an average pulse duration variable that is used to determine the velocity change of the shock pulse according to:

$$\Delta v = 386.4 * A_M * [(T_R/2) + (T_F/2)] \quad (15)$$

where Δv has already been defined,

A_M = maximum-faired acceleration,

T_R = rise time in seconds, and

T_F = fall time in seconds

The half-sine shock pulse produced by the plastic programmers is faired in a similar fashion, as indicated in Figure 8.

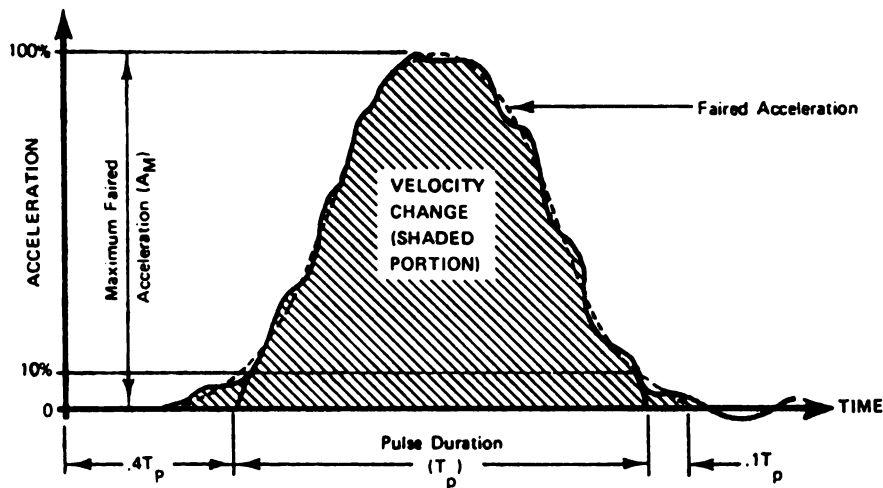


Figure 8. ASTM D 3332 method of fairing a half-sine shock pulse.

The velocity change is determined by

$$\Delta v = 0.636 \cdot A_M \cdot T_p \quad (16)$$

It has been assumed that the high frequency components of a complex wave can be ignored, thus justifying fairing or filtration. This assumption has not been rigorously investigated. It may turn out that high frequency components of a complex wave could have had a detrimental effect on critical elements that have high natural frequencies. These effects would of course be covered up after filtration. Without extensive laboratory investigation, such filtration appears to be unjustified.

The effect of fairing and filtration has also been masked in the shock machine calibration charts. Another problem associated with the use of these calibration charts is that the values listed are valid only for a bare table. As weight is

added to the table, the actual G's that are experienced by both the product and table change, so that a correction factor is needed. The significance of this is that if the correction factor is not applied to the shock machine's calibration chart, then it would appear that the product has a different fragility rating than it really has. As a result, a thinner cushion would be selected and the product would be under-protected, possibly leading to failure.

Another important consideration in fragility testing is the mounting location of the product on the shock table. ASTM D 3332 stresses that the choice of mounting points strongly influences the dynamic response of the product and consequently may affect the fragility rating of a product. This reduces the reliability of the test results.

In view of all of these considerations, possibly erroneous fragility determinations appear to be an inevitable consequence of using the shock machine. Because of these problems, the fragility of a product may be over-estimated, underestimated, or result in an ambiguous value, all of which results in increased cost to the manufacturer.

In addition to all of the problems associated with shock machines, these instruments remain very expensive investments. One manufacturer [Church, 1990] indicated that a small shock machine (65 cm x 81 cm table surface area) equipped with

minimal instrumentation would cost in the range of \$55,000 to \$65,000. As the table size increases and as the instrumentation becomes more sophisticated (signal conditioners, amplifiers, waveform analyzers, etc.), the total cost of a shock machine system can easily be many tens of thousands of dollars more.

These machines also require frequent maintenance that can become expensive. Plastic programmers need to be replaced periodically, as do compression pads, cable wires, and so on. The gas programmers require compressed gas, as do the pneumatic brakes, so gas cylinders need to be refilled. Finally, the machine itself needs to be lubricated and adjusted periodically, requiring the services of a skilled technician.

Since the base of a shock machine is attached to a large seismic mass that is anchored to the floor wherever it is located, shock machines tend to be not very portable. Expensive, dedicated lab space must be set aside for the purpose of maintaining a shock machine, and so is lost for any other purpose. Expensive as this may be, greater costs may be incurred due to the inappropriate use of protective packaging materials, the faulty design of which is a direct consequence of erroneous fragility determinations.

Yet, for all of the problems that are associated with shock machines, shock machines tend to be very popular

instruments. This is a good example of how technical people falsely place their faith in expensive instrumentation without really knowing what it is that the instrument is measuring.

Given all of the problems of a shock machine, it would appear that the acquisition of such a machine for the purpose of DBC determination is a questionable investment. For this reason, an alternative method of determining a product's DBC is presented.

Chapter Two: An Alternative Method for Determining the DBC for a Shock-Sensitive Product

I. The Alternate Method

If one is convinced that their shock-sensitive product can accurately be modeled as in Figure 3, an alternative method to ASTM D 3332 can be used to determine the DBC of the product without requiring the use of a vertical shock machine. As such, this method will be much less expensive because minimal instrumentation is needed for this method.

Since the shock machine will not be used, fragility tests must be conducted by dropping the product onto various surfaces and inspecting for damage. For almost all impact surfaces, the shock produced will be half-sine in shape. This is particularly true for drops onto cushions. The DBC constructed from the results of these drop tests will therefore have the shape shown in Figure 4. Suppose now that a new product with an accelerometer attached to it is dropped onto a very hard surface such as concrete and that this shock just damages a critical element inside the product. From the half-sine shock pulse recorded by the accelerometer, the peak acceleration G and velocity change ΔV may be determined. This gives us one point $(\Delta V, G)$ on the DBC in Figure 4. Next, suppose that another new specimen of the same product is dropped onto a softer surface like a cushion from a much higher height and that this shock also just damages the product. From the accelerometer attached to the product, a second point $(\Delta V, G)$ on

the DBC in Figure 4 is obtained. At this point then, we have only two points in space (on G vs ΔV axes) which we know lie on a curve which has the shape shown in Figure 4.

Before proceeding any further, consider the related results obtained by using the shock machine. The hard surface is replaced by the plastic programmers and the softer surface is replaced by the gas programmer. The results of the drop test also give the same information with the important exception that the two ($\Delta V, G$) points produced when the two new products are damaged are points on the vertical and horizontal lines of the rectangular shaped DBC in Figure 5. The significance of this fact is that at this point, the entire DBC is determined since only two points are required to construct the two lines (one vertical and one horizontal) which form the rectangular DBC. The velocity change from the drop onto the plastic programmers is the critical velocity change and the peak acceleration from the drop onto the gas programmer is the critical acceleration. The critical element properties f_{ce} and G_{cr} then follow directly from equations (13) and (14).

When we now reconsider the results of the drop tests in which we did not use the shock machine, how do we pass a curve with the shape shown in Figure 4 through only two points in space? Since we have no way of knowing whether these points lie on a peak or a trough of the wavy portion of the curve, or even inbetween, it appears that there could be an infinite

number of ways to pass such a curve through two points. This bothersome situation is a direct consequence of the fact that damage was produced with a half-sine shock, hence the shape of the DBC shown in Figure 4. Note that this problem is nonexistent when the shock machine is used since damage is produced with square-wave shocks which leads to the shape of the DBC shown in Figure 5 (no peaks, no troughs, just two straight lines).

As it turns out, the situation is not as hopeless as it seems. Although it may appear that an infinite number of curves with the shape shown in Figure 4 could be drawn through two points, this cannot be the case due to the simple fact that only two parameters, f_{ce} and G_{cr} , determine the shape of the entire DBC. When viewed this way, any point on the curve must contain information about these two parameters. Therefore, if we have two points on the curve, then we must have two separate pieces of information about f_{ce} and G_{cr} . In mathematical parlance, we have two equations in two unknowns. In theory, these two equations may be solve simultaneously for f_{ce} and G_{cr} . Once these parameters are known, the remainder of the half-sine DBC may be constructed as can the entire square-wave DBC!

The first step in the analysis is to use equation(4):

$$G_{ce} = A_m * G_{prod} \quad (4)$$

Since the amplification factor for half-sine shocks (see table in Appendix A or equations(5) and (6)) is a function of frequency ratio only, this can be written more simply as

$$A_m = \text{funct}(f_{ce}/f_{prod}) \quad (17)$$

Solving equation(9) for the duration gives:

$$\text{duration} = 1/(2*f_{prod}) \quad (18)$$

Inserting this into equation(3) gives

$$\Delta v_{prod} = 0.636 * \text{peak acceleration} / (2*f_{prod}) \quad (19)$$

Expressing the peak acceleration in equation(19) in in/sec² and solving for f_{prod} gives

$$f_{prod} = \frac{0.636(G_{prod}^{*386.4})}{2 * \Delta v_{prod}} \quad (20)$$

Sustituting this into equation(17) and simplifying yields

$$A_m = \text{funct} \left[\frac{f_{ce} * \Delta v_{prod}}{123 * G_{prod}} \right] \quad (21)$$

where f_{ce} is in Hz, Δv_{prod} is in in/sec, and G_{prod} is in G's. The argument of the function (the quantity inside parentheses) in equation(21) is just the frequency ratio used to find the amplification factor. As a quick check on the algebraic manipulations up to this point, the values $f_{ce} = 20$ and any choice of values for Δv_{prod} and G_{prod} from the same row in Table 1 may be used in the argument of the function in equation(21).

The result should be the frequency ratio in the same row in Table 1. For example, from the third row of Table 1, $\Delta v_{\text{prod}} = 563$ and $G_{\text{prod}} = 56.5$. The argument in equation(21) then is $(20*563)/(123*56.5) = 1.62$ which is seen to be the frequency ratio (Column 3) in the same row. The result in equation(21) is by no means restricted to the particular critical element parameters used to generate Table 1.

The final step in the analysis is to substitute equation (21) into equation(4) (it should be noted that when the critical element breaks, $G_{\text{ce}} = G_{\text{cr}}$):

$$G_{\text{ce}} = G_{\text{cr}} = G_{\text{prod}} * \text{funct} \left[\frac{f_{\text{ce}} * \Delta v_{\text{prod}}}{123 * G_{\text{prod}}} \right] \quad (22)$$

Equation(22) is the key to constructing the DBC for half-sine and square-wave shocks using only two $(\Delta v_{\text{prod}}, G_{\text{prod}})$ points. This equation provides the shock G_{ce} to a critical element with natural frequency f_{ce} when the product receives a half-sine shock with peak acceleration G_{prod} and velocity change Δv_{prod} . This is a powerful tool for two reasons:

- a) If information about the critical element is available (f_{ce} and G_{cr} are known), then equation(22) may be viewed as a relation between G_{prod} and Δv_{prod} . Combinations of G_{prod} and Δv_{prod} which satisfy this relation form the border of the half-sine damage boundary region.

Hence, equation(22) defines the DBC once f_{ce} and G_{cr} are known.

- b) If information about the critical element is unavailable (typically the case), then f_{ce} and G_{cr} may be deduced by collecting experimental data on two different half-sine shocks which are known to just damage the product: we will call these $(\Delta v_{prod1}, G_{prod1})$ and $(\Delta v_{prod2}, G_{prod2})$. Specifically, f_{ce} and G_{cr} are the solution to the two simultaneous equations below:

$$G_{cr} = G_{prod1} * \text{funct} \left[\frac{f_{ce} * \Delta v_{prod1}}{123 * G_{prod1}} \right] \quad (23)$$

$$G_{cr} = G_{prod2} * \text{funct} \left[\frac{f_{ce} * \Delta v_{prod2}}{123 * G_{prod2}} \right] \quad (24)$$

The solution to equations(23) and (24) for f_{ce} and G_{cr} is difficult since the function referred to here is the complex amplification factor relationship from equations(5) and (6). An iterative solution is required:

Step 1. Guess a value for f_{ce} . Start with 1 Hz.

Step 2. Using the known Δv_{prod} 's and G_{prod} 's for the two shocks which just damage the product, determine the arguments of the function in equations(23) and (24).

Step 3. Using these arguments as frequency ratios, determine the value of the function (the amplification factor A_m) from either equations(5) and (6) or the table in Appendix A.

Step 4. Again, using the known G_{prod} 's, find the predicted value for G_{cr} from equations(23) and (24). The two values for G_{cr} from equations(23) and (24) will in all probability be different (the value for G_{cr} is a fixed number), the guess on f_{ce} in Step 1 must have been wrong.

Step 5. Choose another f_{ce} . Try 2 Hz. Repeat steps 2 through 4 until your guess on f_{ce} produces the same predicted value for G_{ce} from equations(23) and (24).

When the value of f_{ce} is chosen so that the predicted G_{cr} from eqn(23) matches that from equation(24), the iterative solution is complete. The values of f_{ce} and G_{cr} so obtained are the sought after critical element parameters. At this point, the remainder of the half-sine DBC may be constructed either as in Table 2 or as defined by equations(13) and (14). Since the iterative procedure outlined above is tedious and is unlikely to converge to the solution by simple

trial and error guessing on f_{ce} , a program in BASIC has been designed which follows these steps and systematically increases the guess on f_{ce} by small amounts.

The Program in Appendix C begins the search for f_{ce} with an assigned value of 1.00 Hz and continues its search up to 300 Hz in increments of 0.01 Hz (Line 130). This program first requires the operator to input the values of the peak acceleration and product velocity change for both points referred to in equations(23) and (24) (Lines 20, 40, 80, and 100). The corresponding durations are computed (Lines 50 and 110) so that f_{prod} for both points can be determined (Lines 60 and 120). For each guess on f_{ce} (Line 130), A_m is determined for the first f_{ce}/f_{prod} ratio (Lines 140 through 160) using a subroutine which utilizes equations(5) and (6) (Lines 290 through 390). The procedure is repeated for the second ratio (Lines 170 through 190). At this point, the computer makes a determination of whether or not the choice of f_{ce} is indeed the true value of the critical element's natural frequency by examining the absolute value of the difference between $A_{m1} * G_{prod1}$ and $A_{m2} * G_{prod2}$ where A_{m1} refers to the amplification factor associated with the f_{ce}/f_{prod1} ratio of the first data point and A_{m2} refers to the amplification factor associated with the f_{ce}/f_{prod2} ratio of the second data point. Since both numbers represent predictions for G_{cr} , the difference should be zero. Because a zero difference can never be obtained in practice,

a value less than or equal to 0.1 was arbitrarily chosen to end the iteration.

Once f_{ce} has been determined by the condition in Line 200, then G_{ce} is determined in Line 230 by averaging the values of $A_{m1} * G_{prod1}$ and $A_{m2} * G_{prod2}$. Once f_{ce} and G_{cr} are known (Lines 250 and 270), then the procedure used to complete Table 1 will produce the rest of the DBC when half-sine shocks to the product are used in fragility testing. The procedure used to complete Table 2 will produce the square-wave DBC. In the next chapter, simulation test results, sensitivity analysis, the experimental procedure, and concluding comments will be presented.

Chapter Three: Simulation Test Results, Sensitivity Analysis, experimental Procedure, and Concluding Comments

I. Simulation Test Results

The ability of the Program to uniquely determine the natural frequency and fragility of the critical element was tested with data from an expanded version of Table 1 which is shown in Appendix D. Since the half-sine DBC data in Appendix D was derived from a prior knowledge of f_{ce} and G_{cr} , it would appear that deriving f_{ce} and G_{cr} back again from this DBC data is nothing more than a mathematical version of the game "hide and seek". But this is not the case. The purpose of the alternate method presented here is to be able to construct a ABC from limited experimental test results: specifically, from information (G_{prod} and Δv_{prod}) contained in the half-sine shock pulses produced by accelerometers attached to two new products in borderline damage situations. The data in Appendix D should be regarded as experimentally obtained borderline damage results for 50 specimens of the same product in drops onto harder and harder surfaces (as you read down the table). Since the alternate method calls for the destruction of only two new products through impacts (drops) onto two different surfaces, any two of the 50 shocks in Appendix D may be used as fragility test results. Ten different researchers could select twenty different surfaces and get twenty different shocks which just damage the product. In theory, any two of these should determine f_{ce} and G_{cr} . This claim will be put

to the test.

Ten pairs of shocks were taken from Appendix to simulate the results of ten different fragility tests. The results of the Program in Appendix C are shown in Table 4.

Table 4. Ability of the Program to Predict $f_{ce} = 20$ Hz
and $G_{cr} = 100$ G's Using Borderline Damage
Half-Sine Shock Pairs from Appendix D.

Shock Pairs	Predicted f_{ce}	Predicted G_{cr}
12 & 43	19.96	99.97
22 & 48	19.97	99.99
5 & 38	19.96	100.01
8 & 46	19.97	99.98
31 & 50	19.97	99.98
10 & 41	19.96	99.98
19 & 45	19.91	99.72
25 & 35	19.95	100.05
1 & 50	19.96	99.94
24 & 25	19.31	102.19

As demonstrated in Table 4, the Program in Appendix C accurately determines the critical element's natural frequency and fragility when any two points ($\Delta v_{prod1}, G_{prod1}$) and ($\Delta v_{prod2}, G_{prod2}$) on the product's DBC are inserted in the program. It is not necessary that the two shocks correspond to very long and very short duration shocks, as indicated by shock pairs 24 & 25. Shock pairs 1 & 50 test the capability of the program for very long and very short durations, respectively.

The Program was checked for other critical elements to

ensure that it worked for broad ranges of natural frequencies and critical accelerations. The results are presented in Table 5.

Table 5. Ability of the Program to Predict the Properties of f_{ce} and G_{cr} for Various Critical Elements.

Actual f_{ce} (Hz)	Actual G_{cr} (G's)	Predicted f_{ce} (Hz)	Predicted G_{cr} (G's)
2.00	30.00	1.99	30.02
6.00	40.00	5.98	39.998
20.00	10.00	19.63	9.908
100.00	32.00	99.65	31.999
200.00	10.00	197.74	9.99
250.00	250.00	249.69	249.999

Again, the Program accurately predicted the critical element's properties of f_{ce} and G_{cr} over a wide range of values.

II. Sensitivity Analysis

Apparently, any two shocks which just damage the critical element of the product are sufficient to accurately determine the critical element parameters. But what happens if there is an error in either Δv_{prod} or G_{prod} or both? These errors may come from three sources:

i) Instrument Error

ASTM D 3332 requires a maximum error of "5.0%" on all instrumentation (it is not clear whether this is total instrumentation error or error associated with a particular instrument that is used in this standard). It is known that a typical accelerometer has an associated error of $\pm 2.0\%$.

The coupler (a device that amplifies the accelerometer signal) has an error of $\pm 5.0\%$ and an oscilloscope has an associated error of $\pm 3.0\%$. This means that G_{prod} may be in error by as much as $\pm(2.0 + 5.0 + 3.0)\% = \pm 10.0\%$.

ii) Shock Pulse Shape

If damage is produced by drops onto cushions, the shape of the shock pulse may not be a perfect half-sine. In fact, in most situations, it is closer to the "haversine" pulse [Newton, 1976] shown in Figure 9.

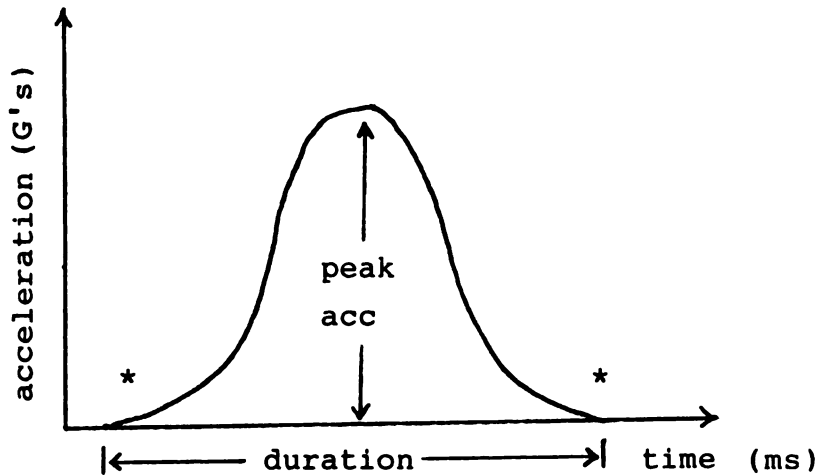


Figure 9. Haversine shock pulse.

The main feature of the haversine pulse is the gradual build up and decline of the acceleration at the beginning and end of the shock pulse (the points marked "*"). The shape factor for the haversine is 0.5 [Newton, 1976] so that the velocity change (equation(3)) is

$$\Delta v = 0.5 * \text{peak acceleration} * \text{duration} \quad (25)$$

in comparison to the half-sine pulse in Figure 1 where the

shape factor is 0.636. The significance of this is that the entire analysis up to this point has assumed that the shape of the shock pulse was half-sine, hence the use of the half-sine shock amplification factors in equations(5) and (6).

It is not known what influence such a pulse may have on the program results for f_{ce} and G_{cr} . The effect may be estimated, however, using a simpler argument: using the half-sine pulse as the basis for discussion, the velocity change for a haversine is $100(0.636 - 0.5)/0.636 = 21.4\%$ smaller than that for a half-sine pulse with the same duration and peak acceleration. The error in assuming that the pulse is half-sine if and when it is in fact haversine may be as much as $1/2 * 21.4 = 10.7\%$. An additional source of error associated with shock pulses of any shape is the determination of the duration itself. It is usually very difficult to tell where a shock pulse begins and ends. This problem affects the ASTM procedure which uses the shock machine as well.

iii) Incorrect Model of Product

If the product cannot be modelled as shown in Figure 3, then the product does not have a DBC. It will be possible in general to produce damage to two new products as outlined here and then plot two points on G vs ΔV axes, but the remainder of the fragility picture cannot be inferred from this information. The purpose of this study was not to address the adequacy of the model but to provide an inexpensive alternative to ASTM D 3332 which like ASTM D 3332 assumes from the start that the product can be modelled as in Figure 3.

Based on reasons i) and ii) above then, the error on both G_{prod} and Δv_{prod} for each of the two shock pulses could be as high as $\pm 10\%$. To see how these errors will influence the f_{ce} and G_{cr} determinations, two arbitrarily chosen shock pairs (12 and 43 from Appendix D) were inserted into the Program after their Δv_{prod} and G_{prod} values were "perturbed" by $\pm 10\%$. For example, in the first entry of Table 5, shock #12 may be perturbed by increasing both the Δv_{prod} and G_{prod} values by 10% and decreasing the values of Δv_{prod} and G_{prod} for shock #43 by 10%. In Table 5, this is indicated as: 12(+10%,+10%) and 43(-10%,-10%).

It should be stressed that a 10% error of Δv_{prod} and G_{prod} values is not a fault of this alternative method, but is a consequence of limitations associated with existing technology (referring to the accuracy of accelerometers, couplers, and oscilloscopes). Since shock machines also use this equipment, the effects of instrument error on f_{ce} and G_{cr} determinations applies equally well to shock machines.

Table 6. Effect on f_{ce} and G_{cr} Determinations When Δv_{prod} and G_{prod} Values of Shock Pairs #12 and #43 from Appendix D Are Perturbed 10%.

Set	Perturbation	Predicted f_{ce}	Predicted G_{cr}
1	12(+10%,+10%) 43(-10%,-10%)	24.20 Hz	104.12 G's
2	12(-10%,-10%) 43(+10%,+10%)	14.46	83.44
3	12(+10%,-10%) 43(+10%,-10%)	16.33	89.98
4	12(-10%,+10%) 43(-10%,+10%)	24.20	109.97
5	12(-10%,-10%) 43(-10%,-10%)	19.96	89.97
6	12(+10%,+10%) 43(+10%,+10%)	19.97	109.98
7	12(+10%,-10%) 43(-10%,+10%)	18.58	87.24
8	12(-10%,+10%) 43(+10%,-10%)	21.51	110.17
9	12(-10%,-10%) 43(+10%,-10%)	15.78	87.50
10	12(+10%,-10%) 43(-10%,-10%)	19.02	86.51
11	12(-10%,-10%) 43(-10%,+10%)	19.32	90.30
12	12(-10%,+10%) 43(-10%,-10%)	25.92	109.14
13	12(+10%,+10%) 43(+10%,-10%)	21.12	108.84
14	12(+10%,-10%) 43(+10%,+10%)	15.81	90.31
15	12(+10%,+10%) 43(-10%,+10%)	23.25	105.74
16	12(-10%,+10%) 43(+10%,+10%)	14.46	83.44

Apparently, the effect of perturbing each of the G and ΔV values used by the Program compounds the errors on f_{ce} by as much as 27.7% (sets 2 and 16) and G_{cr} by as much as 16.6% (also sets 2 and 16).

III. Experimental Procedure

The main difference between the alternative method presented here and the conventional method that uses the shock machine is the technique that is used to generate the shock pulses which just damage the product. In the conventional method, the two shock pulses that just damage the product are of two different forms: a half-sine shock pulse (produced by the plastic programmer of a shock machine) and a "square-wave" shock pulse (produced by the square-wave programmer).

The alternative method uses two half-sine shock pulses to damage the product. For the sake of convenience, it is suggested that one of the shock pulses be of short duration and the other shock pulse be of long duration. The short duration shock is accomplished by simply dropping the product onto a very hard surface, such as a concrete floor. The long duration shock is accomplished by mounting the product on a soft cushion(s) and dropping it onto an immovable surface (again, a concrete floor, for example).

The essential components of this alternative method are described in two ASTM standards: ASTM D 3332 (Method B); and ASTM D 3331 (Assessment of Mechanical-Shock Fragility Using

Package Cushioning Materials), now defunct. ASTM D 3331 was very similar to the procedure outlined here. According to Committee D of ASTM, ASTM D 3331 was likely dropped because there remained an unanswered question as to where the test results were located on the DBC [Church, 1990], and that the utilization of this standard for the purpose of determining the DBC was "... the poor man's method." [Church, 1990]. As demonstrated, determining exactly where the critical acceleration point is located on the DBC is not such a difficult task.

The first drop intended to produce damage to the product should be done by dropping the product onto any hard surface (concrete or steel) at successively higher drop heights until damage occurs. Since the surface is hard, the duration of the shock will be very short and the shock pulse will be reasonably half-sine in shape. The resulting shock pulse is equivalent to the shock pulse produced by the plastic programmers on the shock machine. The velocity change and peak acceleration from the accelerometer are used as the first point used in equation(23).

The next step is to drop a new product onto a surface which will create a relatively long duration shock. The Δv and peak acceleration corresponding to damage in this part of the test are used as the 2nd point in equation(24). The technique suggested for this test is to mount the product on an

assembly of cushions and then drop this product/cushion system onto a hard surface (again, using the concrete floor).

In this scheme, all of the cushions are of the same thickness and made from the same material. The cushion assembly needs to be thick enough so that the product is capable of surviving at least one drop without incurring damage, and each individual cushion needs to be thin enough such that the product will be damaged if the product is mounted on just one of these cushions and dropped from the designated drop height. As such, individual cushions are removed from the assembly with each subsequent drop until damage occurs. Since the area under the shock pulse is equal to the velocity change, and given that the velocity change remains relatively constant (not a strict requirement, but the same drop height would very likely be maintained during this phase of the experiment), then the duration of the shock pulse would decrease and the acceleration would increase, culminating in the failure of the critical element.

Of course, there are other methods that can be used to gradually decrease the pulse duration and increase the acceleration level. Instead of decreasing the thickness of a cushion assembly, drops could be conducted on cushions whose material properties became increasingly stiffer. In this scheme, the cushions are manufactured from different polymer systems.

Another system that could be employed for this phase of

the test would use steel springs, instead of the polymer cushions. A platform constructed of a very stiff material (steel plate, plywood, or other such construction) could be constructed in such a fashion that the platform would be capable of accomodating a number of springs. The initial test would begin with the platform mounted on just a few of these springs, perhaps three or four. After the first drop (and after each subsequent drop), another spring is inserted into the platform until the platform becomes stiff enough to cause an acceleration level that damages the product. The necessary requirement here is that the platform be large enough to accomodate the necessary number of springs that are needed to stiffen the the platform adequately. Alternatively, the springs can be changed with springs whose spring constants are gradually stiffer, until such time that the platform once again becomes stiff enough to cause a shock that damages the product. In the final analysis, it makes no difference how these borderline damage shock pulses are generated as long as they are half-sine in shape.

As a result of these two drop tests, two shock pairs on the product's DBC are identified, $(\Delta v_{\text{prod1}}, G_{\text{prod1}})$ and $(\Delta v_{\text{prod2}}, G_{\text{prod2}})$. After the values of these two shock pairs are inserted into the Program in Appendix C, f_{ce} and G_{cr} are determined. This is the critical information that is needed to determine the remainder of the product's DBC (which can be done by applying equation(22) in conjunction with the procedure

used to construct Table 1 and 2).

A slight complication may arise during the first drop test. Since the product is manually dropped in the alternate method, nearly perfect flat drops will not be possible as with the shock machine. A non-flat drop means that the peak acceleration obtained from the accelerometer will depend on where the accelerometer is attached to the product. This situation is most pronounced when the impact surface is hard. There are two remedies for this.

First, a drop-tester could be deployed during this test. Since drop-testers are capable of producing near-perfect flat drops, this problem is eliminated. However, acquisition, storage, and maintenance costs can be considerable, and the whole point to this thesis is to simplify and reduce the costs associated with fragility testing.

The second solution to this problem is to use cushions during this test. In a non-flat drop onto a soft surface such as a cushion, the surface will deform and contact the entire base of the product. This will usually happen without affecting the motion of the product too much. At this point, the impact is not very much different from a flat drop. Since the Program has been shown to perform very well given any two half-sine shocks, the drop procedure may be modified to replace the drop onto a different cushion or steel spring system.

IV. Concluding Comments

Nearly all of the problems associated with shock machines are thus completely avoided or at least significantly reduced by this alternative method. Most importantly, this method is cost effective. Most of the costs associated with shock machines (purchasing, maintenance, and space requirement costs) are either avoided or significantly reduced. The only equipment and materials needed are an oscilloscope (or waveform analyzer), an accelerometer, cables, couplers, and a cushioning system (polymer cushions or steel spring system, for example). As a result, the fragility testing system discussed here is portable, whereas a shock machine is not.

The fragility testing method discussed here should be capable of determining the fragility of a shock-sensitive product (which meets the classical model requirements) less expensively than when a conventional shock machine system is employed in DBC determinations. Once the fragility of a product has been accurately determined, then protective packaging requirements can be more scientifically determined which leads to decreased packaging costs.

List of References

- 1) Annual Book of ASTM Standards. Volume 15.09. American Society for Testing and Materials. Philadelphia, PA. 1985.
- 2) Brandenburg, R.K. and Lee, J.J.L. Fundamentals of Packaging Dynamics. MTS Systems Corporation. Minneapolis. 1985.
- 3) Burgess, G.J. "Product Fragility and Damage Boundary Theory". Packaging Technology and Science. Volume 1, 1988. Wiley. London.
- 4) Church, E. Telephone conversation April 23, 1990. Lansmount Corporation. Monterey, CA.
- 5) Higdon, A., Ohlsen, E., Stiles, W., Weese, J., and Riley, W., Mechanics of Materials. 1976. Wiley. New York.
- 6) Mindlin, R.D. "Dynamics of Package Cushioning". Bell System Journal. Volume 24, October 1945.
- 7) Newton, R.E. "Fragility Assessment, Theory, and Test Procedure". MTS Systems Corporation. Report 160.06. Minneapolis. 1976.

Appendix A

Shock Amplification Factors for a Half-Sine Pulse

Frequency Ratio f_{ce}/f_{prod}	Amplification Factor A_m
.01	.020
.02	.040
.04	.080
.10	.200
.20	.396
.30	.588
.40	.771
.50	.943
.60	1.102
.70	1.246
.80	1.373
.90	1.482
1.00	1.571
1.10	1.640
1.20	1.690
1.30	1.726
1.40	1.750
1.60	1.768
1.80	1.759
2.00	1.732
2.20	1.694
2.40	1.649
2.60	1.600
2.80	1.550
3.00	1.500
4.00	1.268
5.00	1.083
6.00	1.170
7.00	1.167
8.00	1.126
9.00	1.070
10.00	1.100
11.00	1.100
∞	1.000

Appendix B

Shock Amplification Factors for a Square-Wave Pulse

Frequency Ratio f_{ce}/f_{prod}	Amplification Factor A_m
.02	.063
.04	.126
.10	.313
.14	.436
.20	.618
.26	.794
.30	.908
.36	1.071
.40	1.176
.46	1.323
.50	1.414
.54	1.500
.56	1.540
.58	1.580
.60	1.618
.62	1.654
.64	1.689
.66	1.721
.68	1.753
.70	1.782
.80	1.902
.84	1.937
.88	1.964
.90	1.975
.92	1.984
.94	1.991
.96	1.996
.98	1.999
1.00	2.000
> 1.00	2.000

Appendix C

BASIC Program which determines f_{ce} and G_{ce} from G_{prod} and ΔV_{prod} data.

```

10 PRINT "INPUT GP1";
20 INPUT GP1
30 PRINT "INPUT VEL1";
40 INPUT VEL1
50 DUR1 = VEL1/(GP1*.636*386.4)
60 FP1 = 1/(2*DUR1)
70 PRINT "INPUT VEL2";
80 INPUT GP2
90 PRINT "INPUT VEL2"
100 INPUT VEL2
110 DUR2 = VEL2/(GP2*.636*386.4)
120 FP2 = 1/(2*DUR2)
130 FOR FCE = 1 TO 200 STEP .01
140 RATIO = FCE/FP1
150 GOSUB 290
160 AMP 1 = AMP
170 RATIO = FCE/FP2
180 GOSUB 290
190 AMP2 = AMP
200 IF ABS(AMP*GP1-AMP2*GP2) .1 THEN 230
210 NEXT
220 STOP
230 GCE = (AMP*GP1-AMP2*GP2)/2
240 PRINT "THE NATURAL FREQUENCY OF THE CRITICAL
      ELEMENT IS";
250 PRINT FCE
260 PRINT "THE FRAGILITY OF THE CRITICAL ELEMENT IS";
270 PRINT GCE
280 END
290 REM: AMPLIFICATION FACTOR CALCULATIONS
300 IF ABS(RATIO - 1) .001 THEN RATIO = .999
310 IF RATIO 1, THEN 340
320 AMP = 2*RATIO*COS(3.14159*RATIO/2)/(1-RATIO*RATIO)
330 GOTO 390
340 AMP = 0
350 FOR N = 1 TO (1 + RATIO)/2
360 Q = RATIO*SIN(2*3.14159*N/(RATIO+1))/(RATIO-1)
370 IF Q AMP, THEN AMP = Q
380 NEXT N
390 RETURN

```


Appendix D

Fifty shocks which just damage a product whose critical element has a natural frequency of 20 Hz and a fragility of 100 G's.

Shock Number	Velocity Change (in/sec)	G's
1	5591.67	90.925
2	5449.874	91.346
3	5322.816	92.012
4	5211.748	92.989
5	5023.965	92.578
6	4788.569	91.189
7	4564.891	89.198
8	4352.884	88.751
9	4152.544	87.708
10	3963.915	86.805
11	3787.11	86.063
12	3622.322	85.504
13	3469.862	85.160
14	3330.189	85.067
15	3203.97	85.277
16	3092.161	85.853
17	2996.132	86.884
18	2917.863	88.489
19	2860.261	90.840
20	2724.094	90.735
21	2501.22	87.512
22	2292.283	84.386
23	2096.812	81.362
24	1914.337	78.446
25	1744.385	75.645

Appendix D continued.

Shock Number	Velocity Change (in/sec)	G's
26	1586.493	72.967
27	1440.193	70.421
28	1305.026	68.018
29	1180.533	65.772
30	1066.263	63.699
31	961.773	61.819
32	866.632	60.159
33	780.418	58.751
34	702.730	57.638
35	633.191	56.879
36	571.458	56.551
37	517.236	56.767
38	470.296	57.684
39	439.510	59.540
40	397.888	62.700
41	372.540	67.728
42	353.300	75.228
43	338.802	86.081
44	328.034	101.829
45	320.228	125.265
46	314.780	161.864
47	311.193	223.635
48	309.043	341.929
49	307.500	625.935
50	307.500	1768.097

Appendix E

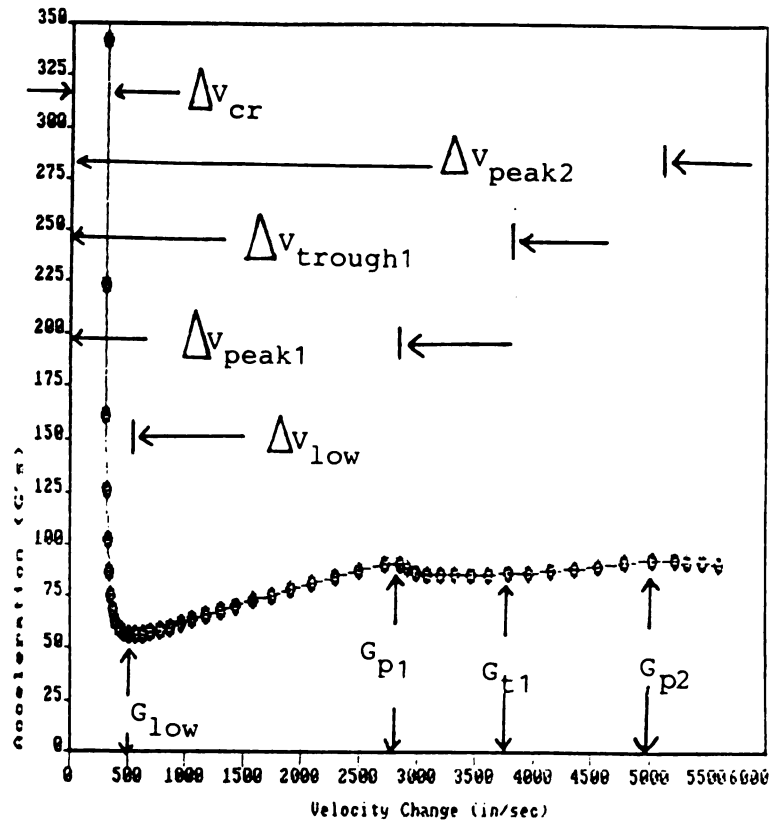
Program 2. This program requires the operator input the critical acceleration and natural frequency of a product's critical element. The program then provides 50 coordinates of a damage boundary curve (for either a half-sine or square-wave shock pulse system) which fully describes the product's damage boundary curve.

```

10 DIM VELCHNG(100),GPRODHS(100),GPRODSQ(100)
20 INPUT F1
30 INPUT GCE
35 REM: GCE IS THE CRITICAL ACCELERATION TO CRITICAL ELEMENT
40 FOR K=1 TO 50
50 TAU2 = 5/F1*((51-K)/50)**1.5
60 F2 = 1/(2*TAU2)
70 RATIO = F1/F2
80 GOSUB 240
90 GPRODHS(K) = GCE/AMP
100 VELCHNG(K) = 245.989*GPRODHS(K)*TAU2
110 Q = (386.4*GCE)/(2*F1*VELCHNG(K))
120 FOR I = 0.01 TO 20 STEP 0.01
130 A = 2*SIN(1.57*I)
140 IF I>1 THEN A = 2
150 IF ABS(A/I-Q)>0.01 THEN 160
153 AMP = A
160 NEXT
170 GPRODSQ(K) = GCE/AMP
175 PRINT VELCHNG(K),GPRODHS(K),GPRODSQ(K)
180 NEXT
190 LPRINT "VELCHNG", "GPRODHS", "GPRODSQ"
200 FOR K = 1 TO 50
210 LPRINT VELCHNG(K),GPRODHS(K),GPRODSQ(K)
220 NEXT
230 END
240 REM: AMPLIFICATION FACTOR CALCULATIONS
250 IF ABS(RATIO - 1) < 0.001 THEN RATIO = .999
260 IF RATIO > 1, THEN 290
270 AMP = 2*RATIO*COS(3.14159*RATIO/2)/(1-RATIO*RATIO)
280 GOTO 340
290 AMP = 0
300 FOR N = 1 TO (1 + RATIO)/2
310 Q = RATIO*SIN(2*3.14159*N/(RATIO + 1))/(RATIO - 1)
320 IF Q > AMP, THEN AMP = Q
330 NEXT N
340 RETURN

```

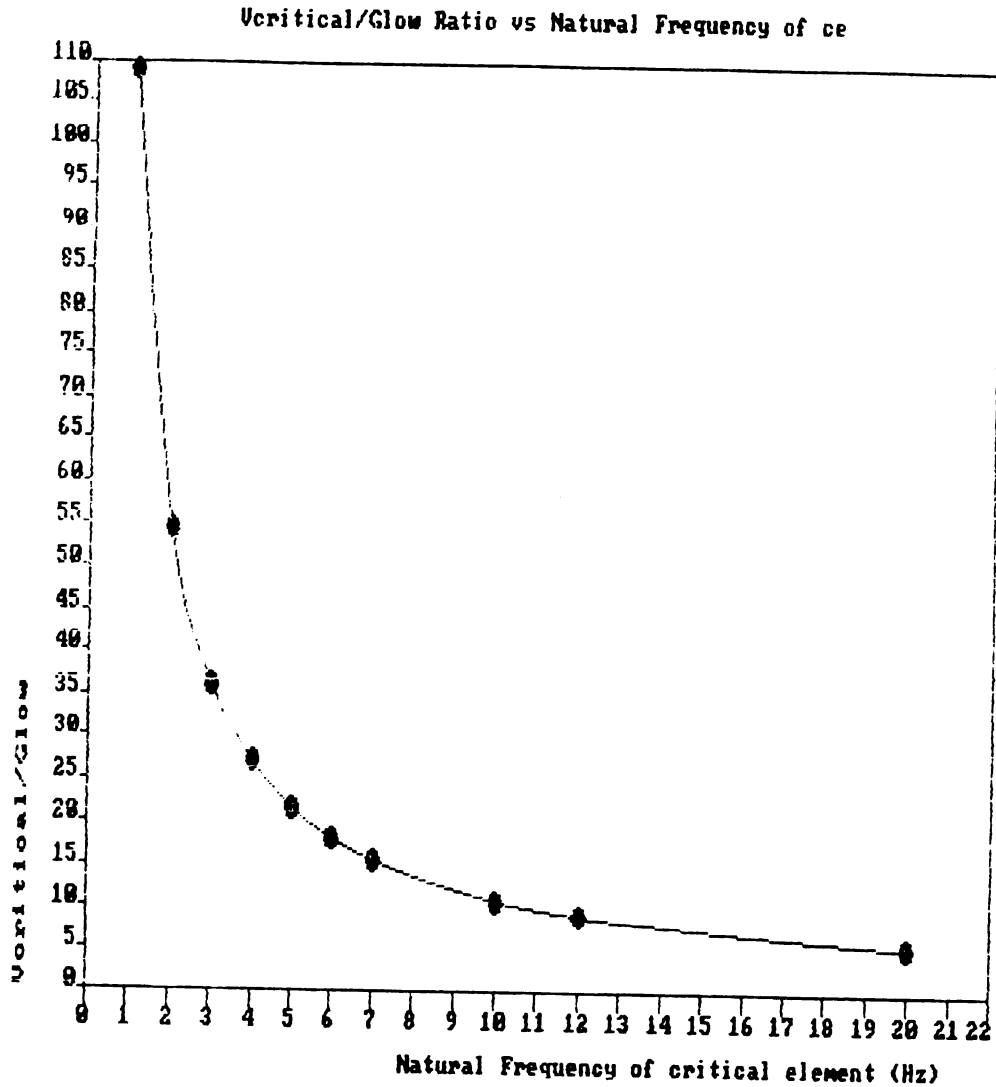
Appendix F



(column b)	(row a)						
	Δv_{peak2}	$\Delta v_{trough1}$	Δv_{peak1}	Δv_{low}	G_{low}	G_{p1}	G_{t1}
Δv_{cr}	16.976	10.8475	9.3168	1.8614			
Δv_{low}	9.12	5.8275	5.0052				
Δv_{peak1}	1.822	1.1643					
$\Delta v_{trough1}$	1.565						
G_{p1}					0.6225		
G_{t1}					0.6648	1.0678	
G_{p2}					0.608	0.9769	0.9148

The DBC parameter ratios listed above are constant for each shock-sensitive product, regardless of what the particular values of of the critical element's natural frequency or fragility rating happen to be.

Appendix G



The relationship between $\Delta V_{cr}/G_{low}$ and the natural frequency of the product's critical element is depicted here. Once two of the three parameters (ΔV_{cr} , G_{low} , or natural frequency) are known, then the remainder of the curve can be deduced using the parameter ratios as shown in Appendix F.

MICHIGAN STATE UNIV. LIBRARIES



31293008761607